Effective Group Potentials. 2. Extraction and Transferability for Chemical Groups Involved in Covalent or Donor−Acceptor Bonds

Romuald Poteau,* Fabienne Alary, Hassna Abou El Makarim,† Jean-Louis Heully, Jean-Claude Barthelat, and Jean-Pierre Daudey

Laboratoire de Physique Quantique, IRSAMC, UMR 5626 du CNRS Université Paul Sabatier, 118 route de Narbonne, 31062 Toulouse Cedex 4, France.

Received: July 12, 2000; In Final Form: September 28, 2000

The effective group potential (EGP) methodology developed in the first article is supported by the idea that some chemical properties of a molecule depend only on a few nuclei and electrons. This technique, which allows one to reduce the number of electrons and nuclei explicitly implied in an ab initio calculation, can be applied to systems which can be separated into an active part and some spectator groups. Chemical groups involved in covalent or donor−acceptor types of bonding have been studied. For example, the silyl group, SiH_3, is replaced by a silicon pseudoatom with only one active electron, and the associated EGP is designed for properly taking into account the electronic effects of the whole fragment on the neighboring chemical group. Three other molecular groups have been replaced by an EGP, namely PH_3, NH_3, and C_5H_5. The latter EGP is designed for a suitable description of the interaction of the π system of the cyclopentadienyl molecule with a metallic atom. The transferability of the EGPs and their usefulness for theoretical calculations on realistic cases are also discussed.

1. Introduction

In the previous paper, we introduced a new method able to reduce the cost of an ab initio calculation. This methodology, called effective group potential (EGP), allows the number of electrons and atomic basis functions to be reduced, without spoiling the description of the electronic structure. It is supported by the analysis that in many chemical processes, some parts of the molecules play a minor role. According to chemical intuition, these parts can be identified as functional groups, such as CH_3, PH_3, CO, ... The keyword "spectator groups" seems suitable for designating chemical groups which do not play an active role in the properties under consideration. However, these groups are important and cannot be substituted by the simple expediency of simulating them by a hydrogen atom. For instance, the milieu in the active site of a protein is determined by the combined effect of all the surrounding chemical groups that could hardly be modeled by hydrogen atoms. The theoretical chemist often takes advantage of this statement by replacing functional groups by simpler systems. For example, it is usual to substitute the methyl group by a less computationally demanding H atom. There have been in the past more spectacular attempts, such as replacing a cyclopentadienyl fragment by a single chlorine atom.[1,2] Other concepts, based upon methodological developments, consist of substituting a molecular fragment by a reduced system with an associated operator, that is, a pseudopotential. All these treatments have a common goal: the reduction of the number of electrons and atomic orbitals without a dramatic loss of accuracy in the electronic description of the active part of a molecule. From a general point of view, the applicability of pseudopotentials is very wide, since it can be used every time that a molecule can be considered as spectator: metal−ligand complexes, adsorption on solids modeled by clusters, reactivity processes, molecules in an inert matrix, etc.

The theoretical background of our EGP method and the recipes for determining an EGP is described in the previous paper. The silyl radical was chosen as an example for exploring the methodology step by step. Derivation of analytic derivatives was also explained, and it was shown that the substitution of functional groups by reduced systems does not significantly affect the potential energy surface (PES) of the active parts.

After giving computational details in section 2, we will check the potentialities of our method on various chemical groups involved in covalent or donor−acceptor complexes such as the silyl radical (section 3) and phosphine and ammonia (section 4). This study also offers an opportunity for giving comments about the transferability. The cyclopentadienyl functional group often present in transition metal complexes, can also be replaced by an EGP developed on a pentagonal pseudosystem (section 5). Moreover, we will show that the EGP provides fair results with second-order Møller−Plesset perturbation theory (MP2), that is, beyond the Hartree−Fock approximation. Finally, the main features of the EGP methodology are recalled, and some perspectives are proposed (section 6).

2. Computational Details

The EGP routines have been included into the Gaussian98 program.[3] As explained in the previous paper, the W_{EGP} operator is expressed as a linear combination of operators:

$$W_{EGP} = \sum_n \sum_m \alpha_{mn} |g_n\rangle\langle g_m| = \sum_n \sum_m \alpha_{nm} W_{EGP}^{nm}$$

where $|g_m\rangle$ designates a Gaussian function. Although it seems analogous to nonlocal atomic effective core potentials (ECPs), it is important to recall that the W_{EGP} operator may be expanded

* Corresponding author. E-mail: romuald.poteau@irsamc.ups-tlse.fr. Fax: (33) 561556065.

† Permanent address: Laboratoire de Chimie Théorique, Faculté des Sciences, Avenue Ibn Batouta, BP1014 Rabat, Morocco.

10.1021/jp002499p CCC: $20.00
Published on Web 12/09/2000

TABLE 1: Truncated Basis Set for the Si#, P#, N#, and Cp# EGPs[a]

chemical group	EGP associated to the pseudogroup *R*	*n*	*l*	exponents	coefficients
SiH_3	$Si^{\#}$	1	0	0.170	1.0
			1	0.160	1.0
PH_3	$P^{\#}$	2	0	0.750	1.0
			1	0.200	1.0
NH_3	$N^{\#}$	2	0	1.000	1.0
			1	0.400	1.0
C_5H_5	$C_5^{\#} \equiv Cp^{\#}$	5	1	0.373	1.0

[a] *n* is the number of electrons on the pseudogroup. The $Cp^{\#}$EGP is expanded on five centers, each one is a pseudo-carbon with one active electron.

on many centers (hereafter called multicentric EGP). Moreover, even one-center EGPs are anisotropic.

During geometry optimizations, the chemical group replaced by an EGP is kept fixed at the value of the reference calculation. All geometrical parameters frozen throughout the optimization process are indicated by an asterisk in the tables.

We used the Durand and Barthelat atomic pseudopotentials[4] expressed in a nonlocal formulation, except for the transition metals, i.e., niobium and tantalum. In that case, small core semilocal pseudopotentials were used to replace the 28 and 60 core electrons for Nb and Ta, respectively.[5] Atomic pseudopotentials include relativistic effects for elements heavier than argon. All the Gaussian basis sets are of double-ζ plus polarization quality[6] unless otherwise mentioned.

3. An Example of Covalent Bond: SiH_3

3.1. Choice of the Reference Molecule. We indicated in the first paper that the silyl molecular fragment (SiH_3) was chosen to illustrate the ability of our method to replace properly a chemical group involved in a covalent bond by an EGP. This choice is motivated by future applications in the field of chemical surfaces.

The reference system is the disilane molecule, which is reduced to SiH_3R where *R* is at the same place as the silicon atom of the substituted silyl functional group. It supports a part of the *truncated basis set* $\{f_p\}$, while the basis set on SiH_3 remains unchanged. The exponents of *R* which ensure a good agreement between molecular valence pseudoorbitals (MVPO, see paper 1) and reference MOs are recalled in Table 1. Two EGP operators were designed (see paper 1), the first one (EGP_1) is a one-center pseudopotential which approximately fits the reference calculation, while the second one (EGP_2) is a many-center pseudopotential which fits the reference molecular orbitals perfectly. However, we have shown that the latter operator does not very accurately reproduce the optimal geometry and the force constants of the active part (namely SiH_3) in the reduced disilane molecule.

3.2. Transferability. To be useful, the EGPs must be transferable to other molecules. We hope that the pseudopotential is at least transferable when the pseudoatom is linked to another atom belonging to the same group of the periodical classification. Three criteria are considered for checking the validity of the EGPs with regard to a full calculation on CH_3SiH_3: the MO energies and shapes must be in good agreement; the optimal geometry must be analogous in both cases; the sensitivity of the energy to geometric deformations of the CH_3 fragment must be almost identical.

The energies of the occupied and virtual MOs are displayed in Figure 1. In the case of $Si^{\#}$ EGP_1, the spectrum of $CH_3Si^{\#}$ is slightly shifted toward higher values with respect to the CH_3-SiH_3 one. The HOMO stands at −0.42469 hartree instead of −0.45734, while the $Si^{\#}$ EGP_2 yields −0.48566 hartree. Moreover, the shapes of the MOs implied in the C−H and C−Si bonding are in good agreement with both EGPs.

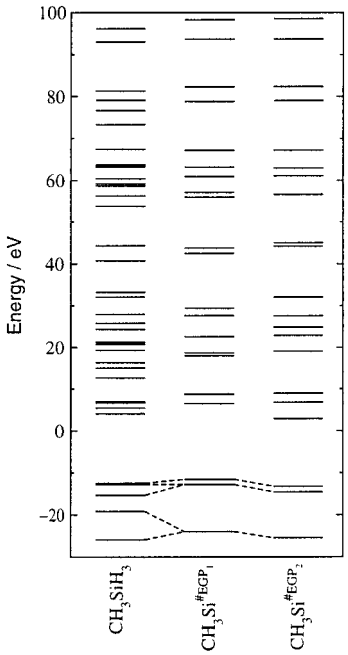

Figure 1. Energy of the MO of CH_3SiH_3 and $CH_3Si^{\#}$ in their respective optimal geometry (hartree). The dashed lines correlate occupied orbitals with analogous character.

TABLE 2: Geometrical Parameters (Distances in Angstroms and Angles in Degrees) for the CH_3SiH_3 and $CH_3Si^{\#}$ Structures (C_{3v}) at the HF Level of Calculation[a]

	CH_3SiH_3	$CH_3Si^{\#}$ EGP_1		$CH_3Si^{\#}$ EGP_2		
C−Si	1.877	1.877*	1.800*	1.950*	1.877*	2.348*
C−H	1.094 (5.73)	1.095 (5.68)	1.097	1.093	1.146 (5.17)	1.107
HCSi	111.1 (0.82)	112.8 (0.95)	113.8	112.0	120.3 (1.73)	101.9
Si−H	1.477					
HSiC	110.6					

[a] Force constants are indicated in parentheses (stretching mode in mdyn·Å^{-1} and bending mode in mdyn·Å·rd^{-2}). The asterisk * means that the geometrical parameter is frozen throughout optimization.

However, the influence of the two $Si^{\#}$ EGPs on the geometry of the CH_3 molecular group is not comparable. The full optimization of CH_3SiH_3 provides a C−Si distance of 1.877 Å (see Table 2). This parameter has been frozen to the same value in both EGP calculations. From the results reported in the table, it can be shown that the $Si^{\#}$ EGP_2 is disqualified. The C−H bond length is 0.05 Å longer, and the HCSi angle is 9° bigger, while the $Si^{\#}$ EGP_1 has a better influence on the geometry of CH_3. As a matter of fact, in that case the bond length and the angle are only 0.001 Å and 1.7° higher. We also attempted to freeze the C−$Si^{\#}$ bond length to 2.348 Å, that is the distance of extraction of W_{EGP}, in the case of the EGP_2 operator. The implicit purpose is to put the sites of this multicentric EGP into coincidence with the atoms of the active part, contrary to the previous use of that pseudopotential. The angle is now 9° smaller than expected. The $Si^{\#}$ EGP_2 is quite disappointing. A plausible explanation is that due to its multicentric shape, this pseudopotential is too strongly dependent on the nature and on the location of its neighboring atoms. In contrast, the $Si^{\#}$ EGP_1 is also able to take account of the deformation of the CH_3 molecular group as can be seen from the force constants reported in Table 2.

TABLE 3: Geometrical Parameters and Force Constants for Si_2H_6 (D_{3d}) and CH_3SiH_3 (C_{3v}) at the MP2 Level of Calculation (Units: Same Convention as in Table 2)

	Si_2H_6	$SiH_3Si^{\#}EGP_1$		CH_3SiH_3	$CH_3Si^{\#}EGP_1$
Si−Si	2.329	2.329*	C−Si	1.875	1.875*
Si−H	1.474 (3.11)	1.480 (3.04)	C−H	1.100(5.57)	1.101 (5.53)
HSiSi	110.1 (0.68)	112.9 (0.77)	HCSi	111.1 (0.75)	113.5 (0.89)

3.3. Discussion. Considering all these results, it can be assessed that our methodology gives very promising results. The EGP seems to be a good approximation for obtaining various properties: geometrical parameters, charge transfer, monoelectronic spectrum and MOs (see also paper 1). Not only is the $Si^{\#}$ one-center EGP able to reproduce the electronic effect of a chemical group in a given molecular neighborhood, but it is also significantly transferable to other molecules. As concerns the specific case of the $Si^{\#}$ EGP, it can be an interesting tool for ab initio studies of organosilicon compounds, hydrogenated silicon clusters, or adsorption on silicon clusters. Nevertheless, the distance between the $Si^{\#}$ EGP and its first neighbor cannot be optimized, as it was mentioned in the first paper. It is thus important to have a good idea of that bond length. In the $CH_3Si^{\#}$ case, the $C-Si^{\#}$ distance was set to the optimized value in methylsilane, but it is obvious that it will not be possible to do a full reference calculation in realistic applications of the EGP methodology. Now, structural databases provide information on crystalline organic compounds. It can be found in the *Handbook of Chemistry and Physics*,[7] for example, that the mean C−Si distance varies from 1.837 to 1.888 Å according to the kind of neighbors and the hybridization of C and Si. It is therefore possible to estimate a reasonable C−Si distance from these data. However, one has to verify that a slight modification of the $C-Si^{\#}$ distance with respect to 1.877 Å does not dramatically change the geometry of the methyl fragment. We have thus undertaken complete optimizations of CH_3 with two different frozen $C-Si^{\#}$ distances which enclose 1.877, i.e., 1.800 and 1.950 Å (see Table 2). While the C−H bond length is almost insensitive to that modification, the angle undergoes a small variation of 0.8°. This modification is not very important if one considers that the $C-Si^{\#}$ limit values are beyond the mean values reported in structural databases.

3.4. Second-Order Møller−Plesset (MP2) Calculations. Of course, the Hartree−Fock method suffers limitations, and in many cases it is necessary to improve the HF wave function by inclusion of electronic correlation effects. On the other hand the calculation of excited states involves a configuration interaction (CI) treatment. We consider preliminary calculations at the MP2 level of theory as a first step toward the use of EGP in the framework of correlated methods. The geometries of Si_2H_6 and CH_3SiH_3 have been optimized at the MP2 level of calculation. The force constants have also been computed. These results given in Table 3 are compared with those obtained when one SiH_3 fragment is replaced by the $Si^{\#}EGP_1$. While the Si−H bond length is almost the same with respect to the HF calculation, the C−H bond slightly increases. This trend is observed with both the full molecule and the reduced system. As concern the angles, while they are not modified at the MP2 level of theory, they increase by approximately 0.5° for both reduced systems, which is not significant. The force constants are equivalent, the largest error concerns the angular one, just as in the HF calculations. Thus, there are no major discrepancies. Insofar as the second-order terms of the perturbation expansion involve the virtual orbitals and their monoelectronic energies, it means that although the EGP parameters are determined from the valence spectrum only, the virtual MOs are also well reproduced.

TABLE 4: Geometrical Parameters and Force Constants for CF_3SiH_3 (C_{3v}) and CF_2HSiH_3 (C_s) at the HF and MP2 Levels of Calculation (Units: Same Convention as in Table 2)[a]

	HF		MP2	
	CF_3SiH_3	$CF_3Si^{\#}EGP_1$	CF_3SiH_3	$CF_3Si^{\#}EGP_1$
C−Si	1.934	1.934*	1.933	1.933*
C−F	1.336 (6.54)	1.336 (6.48)	1.374 (4.98)	1.375 (4.84)
FCSi	112.3 (2.03)	112.9 (2.13)	112.1 (1.81)	113.0 (1.90)
H−Si	1.465		1.467	
HSiC	107.0		107.0	

	HF		MP2	
	CF_2HSiH_3	$CF_2HSi^{\#}EGP_1$	CF_2HSiH_3	$CF_2HSi^{\#}EGP_1$
C−Si	1.918	1.918*	1.918	1.918*
C−H	1.089 (5.84)	1.085 (5.96)	1.102 (5.42)	1.098 (5.51)
C−F	1.362 (5.92)	1.365 (5.67)	1.399 (4.72)	1.405 (4.61)
HCSi	114.0 (1.22)	116.3 (1.28)	115.0 (1.08)	117.3 (1.16)
H−Si	110.9 (1.59)	111.3 (1.71)	110.3 (1.40)	111.3 (1.54)
FCSi	1.468		1.468	
H−Si	1.469		1.470	
H−Si[a]	108.8		108.1	
	107.6		107.9	

[a] Geometrical parameters of the two hydrogen atoms symmetrically equivalent.

3.5. Robustness. The $Si^{\#}$ EGP was extracted from a system with no charge transfer between the active and spectator part, the disilane molecule. Its transferability has then been checked on an organosilicon compound, CH_3SiH_3, in the framework of both HF and MP2 methods. The aim of the following study is to estimate the behavior of the EGP when confronted with a very polar fragment, namely CF_3. The HF and MP2 geometrical parameters and force constants of CF_3 submitted to the influence of the silyl chemical group and the $Si^{\#}$ EGP, respectively, are reported in Table 4. As usual, the $C-Si^{\#}$ distance is frozen. The C−F bond length is almost identical in both cases. As concerns the FCSi angle, the agreement is satisfying. Another point concerns the intrinsic symmetry of the W_{EGP} operator. As it was extracted from a molecule with a 3-fold symmetry axis, its use on a less symmetrical molecule is questionable. The geometrical optimization of CF_2HSiH_3 has been performed in order to detect a possible artifact. As seen from the table, both distances and angles are preserved with the EGP, with respect to the calculation of the complete molecule. As for the force constants, a careful reading of the results given in this table does not reveal discrepancies.

Finally, we have also investigated the structural and electronic properties of a small hydrogenated silicon cluster, Si_5H_{12}. The Si_nH_m clusters have recently been the object of many theoretical works,[8] after the discovery of intense photoluminescence emission in porous silicon,[9] As a matter of fact, experiments suggest that the luminescence is due to the presence of highly hydrogenated nanoclusters with local ordering domains.[10] Most of the theoretical works focus on the geometrical properties and the energy gaps of small H-passivated silicon clusters. The goal of this contribution is to show that a $Si^{\#}$ could be helpful in first-principles calculations on such systems. Moreover, we will show that the use of three $Si^{\#}$'s in the same molecule does not affect the good behavior which was previously underlined.

In the Si_5H_{12} cluster, one atom of silicon is tetrahedrally coordinated with four SiH_3 groups (Scheme 1). We did not perform a full geometry optimization; the SiH_3 fragments are frozen at the geometry they adopt in the disilane molecule. Moreover, three Si−Si distances are frozen to 2.359 Å, i.e.,

SCHEME 1: T_d Structure

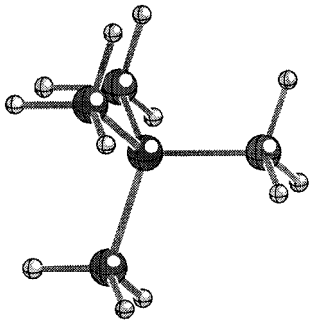

SCHEME 2: C_{3v} Structure

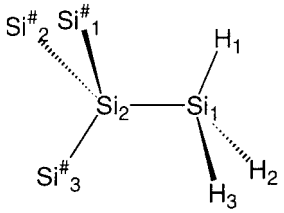

TABLE 5: Geometrical Parameters and Force Constants for the Si_5H_{12} (C_{3v}) Molecule at the HF and MP2 Levels of Calculation (Units: Same Convention as in Table 2)

	HF		MP2	
	Si_5H_{12}	$SiH_3SiSi_3^{\#}$ EGP_1	Si_5H_{12}	$SiH_3SiSi_3^{\#}$ EGP_1
Si_1Si_2	2.357 (1.84)	2.322 (1.91)	2.329 (1.86)	2.310 (1.95)
HSi_1	1.476 (3.16)	1.489 (2.94)	1.475 (3.10)	1.488 (2.91)
HSi_1Si_2	110.2 (0.74)	113.7 (0.80)	110.1 (0.70)	114.0 (0.81)

the experimental Si−Si bond length in the crystal. We want to have a quantitative indication of the influence of the environment on one remaining SiH_3 group. Therefore, three silyl fragments are considered as spectator groups, and replaced by the $Si^{\#}$ EGP_1 (Scheme 2). Eighteen electrons and 72 basis functions are removed. Both theoretical treatments yield very similar results, although the minima are slightly shifted by 0.02 and 0.01 Å for the Si−Si and Si−H bond lengths, respectively, and by 3.5° for the HSiSi angle (see Table 5). The HOMO−LUMO gap is 13.5 eV for Si_5H_{12},[8c] while it is found to be 14.5 eV in the EGP calculation. This apparent discrepancy is not so surprising, since it has been noted in ref 8c that in Hartree−Fock calculations, the gap is strongly dependent on the quality of the atomic basis set. The difference between two basis sets may attain 2 eV. Hence, we estimate that the difference between the two treatments, that is, with and without EGP's, is rather small.

4. Two Examples of Lewis Bases: PH_3 and NH_3

4.1. Extraction of the EGP Operator. Phosphine (PH_3) and ammonia (NH_3) are representative Lewis bases. As a matter of fact, the N and P atoms possesses a donor electron pair. The two hydrides do not present the same geometrical or basicity properties.[11−13] Hence, the HNH angle is approximately 13° higher than the HPH angle and NH_3 forms the stronger bond with an acceptor.[12] We focus our attention on the electronical and geometrical properties of adducts such as AH_3ZH_3 (Scheme 3). From now on, the A and Z letters will indicate an acceptor atom (i.e., gallium or boron) and a donor atom (nitrogen or phosphorus), respectively. The $Z^{\#}$ EGP has been extracted from the BH_3ZH_3 molecule. Ab initio calculations were performed in a smaller basis set than in the disilane case. Indeed, the basis set on the H atoms is a double-ζ 4s/2s basis (s exponents are identical to those used for the calculations on disilane).

SCHEME 3: C_{3v} Structure (Z = P or N, A from Group 13)

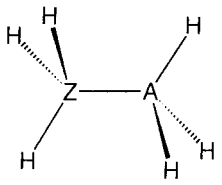

TABLE 6: Geometrical Parameters for the BH_3ZH_3 Structure (C_{3v}) (Units: Same Convention as in Table 2)

	BH_3PH_3	$BH_3P^{\#}$
BP	2.037	2.037*
BH	1.215	1.233
HBP	102.6	101.8
PH	1.412	
HPB	117.6	

	BH_3NH_3	$BH_3N^{\#}$	exp[14]
BN	1.700	1.700*	1.658
BH	1.219	1.231	1.216
HBN	104.0	103.2	104.7
NH	1.011		1.014
HNB	111.2		110.3

TABLE 7: HF Energies (Hartree) of the MOs for BH_3ZH_3, BH_3R, and $BH_3Z^{\#}$

main character of the MO	BH_3PH_3	BH_3R	$BH_3P^{\#}$
B−P (and B−H)	−0.43350	−0.43587	−0.43278
B−H	−0.43438	−0.44902	−0.42477
B−H	−0.43438	−0.44902	−0.42477
P−H	−0.58451		
P−H	−0.58451		
B−H (and B−P)	−0.68582	−0.69791	−0.69871
P−H	−0.92376		

main character of the MO	BH_3NH_3	BH_3R	$BH_3N^{\#}$
B−H	−0.41189	−0.42903	−0.42005
B−H	−0.41189	−0.42903	−0.42005
B−N and B−H	−0.50502	−0.50542	−0.49706
B−N and B−H	−0.70339	−0.73192	−0.74653
N−H	−0.72550		
N−H	−0.72550		

The structural parameters of the reference molecule are reported in Table 6. Experimental gas-phase data are only known for BH_3NH_3,[14] and they are also indicated in the table. BH_3ZH_3 belongs to the C_{3v} symmetry group, and has a staggered conformation. The B−N bond length is 0.34 Å shorter than the B−P distance, while the HBZ angle and B−H bond length are similar in both molecules. The HF canonical MOs of BH_3ZH_3 are already localized on each moiety and on the B−Z bond, and it is straightforward to identify two degenerate B−H MOs and two mixed B−H and B−Z MOs from which the effective MOs will be deduced (see Table 7). In both cases, the ZH_3 fragment is reduced to a two-electron pseudogroup R with one s and one p shells (see Table 1). As usual, the exponents are adjusted in order to reproduce the net charge transfer between ZH_3 and BH_3 (the Mulliken population analysis is presented in Table 8). It is then checked that the effective MOs do have the main features of the four B−H and B−Z orbitals, and that their monoelectronic energies are analogous (see Table 7, column BH_3R).

It is interesting to notice that the two BH/BN orbitals in BH_3NH_3 are lower than the pure B−H MOs, while in the BH_3PH_3 molecule, the highest orbital has BH/BP character and

TABLE 8: Mulliken Population Analysis for BH_3ZH_3, BH_3R, and $BH_3Z^{\#}$

BH_3PH_3	BH_3R	$BH_3P^{\#}$
B: 3.002	B: 3.078	B: 3.163
H: 1.076	H: 1.059	H: 1.033
PH_3: 7.767	R: 1.745	$P^{\#}$: 1.737
BH_3NH_3	BH_3R	$BH_3N^{\#}$
B: 2.954	B: 2.941	B: 3.105
H: 1.115	H: 1.119	H: 1.074
NH_3: 7.699	R: 1.699	N^{*}: 1.672

TABLE 9: s and p Parameters Used for the Determination of the Nonlocal Potentials for $P^{\#}$ and $N^{\#}$ [a]

exponents
7.0000
3.5000
1.7500
1.1670
0.7780
0.5185

[a] The Gaussian functions are located on the P and N atoms, respectively.

is almost degenerate with the BH MOs. It is desirable that the operator could approximately reproduce these features. The conclusions stated from the disilane study encouraged us to build a one-center pseudopotential. The set of exponents is indicated in Table 9. It was found that six s and six p Gaussian functions are needed for a rather good reproduction of the characteristics of the fictitious system. It is necessary to point out that the choice of the basis set of the fictitious atom and of the operator was directed by the transferability of the EGP. This point will be discussed in the next paragraph. The present $Z^{\#}$ EGP is considered as the best compromise between the reproduction of the electronic properties of the reference molecule and the transferability of the operator.

The overall agreement between the full calculation and the reduced one is slightly better than in the disilane case. As concerns the monoelectronic energies, the average error is approximately 0.01 hartree. The largest discrepancy is observed for the N−B MO energy (0.04 hartree), but it does not modify the relative ordering of the MOs. The quasi-degeneracy of the three highest MOs of BH_3PH_3 yield to a switch of the BP and BH MOs. A full optimization of BH_3ZH_3 has been performed in order to show that the $Z^{\#}$ EGP does not alter the geometry of the BH_3 fragment (see Table 6). As a matter of fact, the agreement is quite good; the error on the bond lengths is 0.02 Å, while the angles differ by no more than 0.8°.

4.2. Transferability. The $N^{\#}$ and $P^{\#}$ EGP's were extracted from the BH_3ZH_3 molecule, and their transferability is checked for 10 adducts of the type AH_3ZH_3 (A belongs to group 13, A = B, Al, Ga, In, Tl and Z belongs to group 15, Z = N, P). All the adducts are assumed to have a staggered conformation and C_{3v} symmetry. The A−H bond lengths, ZAH angles, and the corresponding force constants obtained at the HF and MP2 levels of theory are displayed in Tables 10 and 11, respectively. The $A-Z^{\#}$ distance was frozen to the same value as in the optimized AH_3ZH_3 molecule.

4.2.1. HF Calculations. In the case of BH_3PH_3 vs $BH_3P^{\#}$, the error on the B−H bond length is 0.02 Å, that is, larger than the error on the Si−H bond length (0.005 Å) in $SiH_3Si^{\#}$ (EGP_1). Moreover, the HF bending PBH force constant is underestimated by 34% (Table 10), and the $BH_3P^{\#}$ HOMO is not the expected MO mainly built on boron and phosphorus. The two highest occupied MOs are actually inverted (Table 7). Thus, it could be concluded that the $P^{\#}$ EGP is not correct. However, the geometries of the five $AH_3P^{\#}$ molecules are in reasonable agreement with the full calculation: the average error on the A−H bond lengths and HAP angles is rather small. As for the force constants, the largest error are obtained for the HAP angular one (12%). The removal of that case from the statistical set yield an error equals to 5.6%. One can notice the same trends for the AH_3NH_3 molecules. A comprehensive study of these results pleads in favor of the present $N^{\#}$ and $P^{\#}$ EGP. It is important to underline the difficulty for extracting an EGP, and that the choice of the reference molecule can yield artifacts. As a matter of fact, another $P^{\#}$ EGP did not succeed with respect to the transferability criterion. In that case, we have assumed that due to the average location of gallium in the group 13, the GaH_3PH_3 should have been a good candidate as the reference molecule. A p shell on the fictitious phosphorus atom and a 4s4p operator seemed adequate. The difference on the Ga−H bond length and the PGaH angle were less than 0.001 Å and 0.5 Å respectively, and the errors on the corresponding force constants were approximately 2% and 13%. The transferability on the InH_3PH_3 and TlH_3PH_3 adducts appeared very good, and the discrepancy between full calculations and calculations involving that $P^{\#}$ EGP was very small. Nevertheless, the agreement on the force constants was less convincing: 1.5% on the AH stretching force constants, but 15% on the bending constants, with a surprising 38% for the $TlH_3P^{\#}$ adduct. Moreover, the performance of that EGP has broke down for boron and aluminum adducts, particularly as concerns the influence of the EGP on the geometry of the acceptor molecule

TABLE 10: Geometrical Parameters and Force Constants of the AH_3ZH_3 Adducts, HF Calculation (Units: Same Convention as in Table 2)

		A−H		ZAH	
A	A−P	AH_3PH_3	$AH_3P^{\#}$	AH_3PH_3	$AH_3P^{\#}$
B	2.037	1.215 (3.72)	1.233 (3.38)	102.6 (0.73)	101.8 (0.48)
Al	2.617	1.599 (2.21)	1.608 (2.12)	97.3 (0.49)	98.2 (0.44)
Ga	2.739	1.579 (2.21)	1.586 (2.12)	96.0 (0.48)	97.1 (0.45)
In	2.897	1.747 (1.95)	1.754 (1.88)	95.6 (0.43)	96.7 (0.41)
Tl	3.207	1.730 (1.91)	1.734 (1.88)	93.0 (0.40)	94.1 (0.40)
		A−H		ZAH	
A	A−N	AH_3NH_3	$AH_3N^{\#}$	AH_3NH_3	$AH_3N^{\#}$
B	1.700	1.219 (3.63)	1.231 (3.44)	104.0 (0.92)	103.2 (0.66)
Al	2.090	1.606 (2.15)	1.615 (2.09)	99.4 (0.61)	99.0 (0.50)
Ga	2.195	1.586 (2.15)	1.594 (2.09)	98.5 (0.59)	98.7 (0.51)
In	2.378	1.754 (1.90)	1.759 (1.87)	97.4 (0.50)	97.7 (0.44)
Tl	2.622	1.735 (1.87)	1.739 (1.84)	95.0 (0.46)	95.6 (0.44)

TABLE 11: Geometrical Parameters and Force Constants of the AH_3ZH_3 Adducts, MP2 Calculation (Units: Same Convention as in Table 2)

		A−H		ZAH	
A	A−P	AH_3PH_3	$AH_3P^{\#}$	AH_3PH_3	$AH_3P^{\#}$
B	1.961	1.220 (3.64)	1.243 (3.25)	103.4 (0.68)	101.3 (0.29)
Al	2.557	1.608 (2.13)	1.620 (2.01)	97.1 (0.46)	98.4 (0.38)
Ga	2.637	1.593 (2.09)	1.603 (1.99)	96.2 (0.45)	97.9 (0.40)
In	2.828	1.762 (1.84)	1.771 (1.77)	95.4 (0.40)	97.2 (0.37)
Tl	3.073	1.751 (1.76)	1.756 (1.71)	93.2 (0.38)	94.9 (0.38)
		A−H		ZAH	
A	A−N	AH_3NH_3	$AH_3N^{\#}$	AH_3NH_3	$AH_3N^{\#}$
B	1.672	1.225 (3.55)	1.235 (3.42)	104.3 (0.85)	103.2 (0.59)
Al	2.087	1.615 (2.07)	1.622 (2.01)	99.3 (0.56)	98.8 (0.47)
Ga	2.170	1.599 (2.04)	1.606 (1.99)	98.6 (0.54)	98.8 (0.47)
In	2.365	1.769 (1.81)	1.773 (1.77)	97.3 (0.46)	97.7 (0.41)
Tl	2.583	1.756 (1.71)	1.758 (1.70)	95.2 (0.43)	95.9 (0.41)

SCHEME 4: C_s Structure

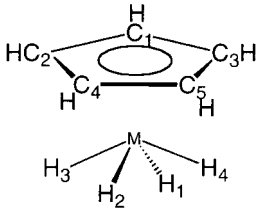

(up to 8° of variation for the AlPH angle). The justification is that we did not take into account that the strongest bond is formed with BH_3, and that the description of the B−P bonding may demand a somewhat different description than the Ga−P bond. Despite the efforts made for designing a suitable operator, it appeared that the definition of an s orbital on the pseudo-phosphorus atom was the only way to get a trustworthy EGP.

This remarkable case shows that the EGP's must be extracted cautiously and that the transferability must be checked on various systems in order to be sure that the reduced basis set on the pseudoatom is adequate. In the PH_3 or NH_3 case, the difficulty for extracting a reliable EGP is linked to the controversial nature of the electronic structure of donor−acceptor complexes: is the donor−acceptor bond mainly caused by electrostatic interactions or are covalent contributions dominant? For example, an analysis of the electronic structure using the natural bond orbital partioning scheme (NBO) suggests that the strongly bound boron complex BH_3 NH_3 has a significant covalent contribution, while the very strongly bound complex $Me_3N-AlCl_3$ is mainly bound by electrostatic contributions.[10]

4.2.2. MP2 Calculations. There is a good overall agreement between the results of the AH_3ZH_3 reference adducts and of the $AH_3Z^{\#}$ model molecules (Table 11). There is no significant increase of the average errors in the geometrical parameters and the force constants with respect to HF calculations, except for $BH_3Z^{\#}$. In particular, the HBP force constants are underestimated. The bending mode is too soft and the error is now greater than 50%. Thus, the perturbation treatment of the correlation energy has increased the discrepancy already observed in HF calculations, while the BHN force constant error is almost the same. A careful analysis of the bonding in the phosphine-borane complex is certainly needed in order to understand the origin of this problem.

5. An Example of π-Donor Group in a d-Metal Complex: The Cyclopentadienyl

5.1. Extraction of the EGP Operator. The cyclopentadienyl ligand C_5 H_5 (abbreviated as Cp) is one of the most common ligands encountered in modern organometallic chemistry. The $Cp^{\#}$ EGP was extracted from a $(C_5H_5)TaH_4$ complex (Scheme 4) where the Cp^- ligand is the electronic equivalent of three simple Lewis bases.[15] Allowing for the fact that a Cp ligand, in such an η^5 complex, forms three bonds to the metal, this type of complex, in which six p electrons are involved, is seven coordinated and possesses a geometry close to the piano-stool structure reported by Kubacek et al.[16] Details of the bonding of Cp in such complexes have been already described. Here, we just specify that in our work the $CpTaH_4$ complex possesses 42 valence electrons accommodated by filling 21 MOs. Ten of them describe the σ skeleton of the Cp ligand, four the inner shells of tantalum, and seven the bonding MOs between the metal and the ligands. The 11 MOs of interest are reported in the first column of Table 12. They correspond to the bonding we want to reproduce with an effective group potential. Thus, the Cp ligand is reduced to a chemical fragment bearing five electrons. All the electrons which are involved in σ_{C-H} and σ_{C-C} bonds are removed. A localization procedure is also applied to the system. It allows us to select only those MOs involved in the binding of the TaH_4 fragment with the π donor orbitals of Cp. The (C_5 H_5) functional group is thereby reduced to a five-center pseudogroup R_5, the position of each R coinciding with a carbon of the reference group.

As for the previous systems, the optimal geometry of the model system was used as reference. Details of the geometrical structure are given in Table 13 for the Cp part, and in the first column of Table 14 for the TaH_4 part. As can be seen in Table 13, the Cp structure exhibits slight deformations with respect to a perfect pentagon. Information about molecular orbitals and Mulliken charges is presented in the first columns of Tables 12 and 15, respectively.

It must be underlined that unlike the previous EGP's, this potential is multicentric, i.e., expanded on five centers noted $C^{\#}$. The basis set associated with each $C^{\#}$ is given in Table 1. Many tests were performed to determine the best *truncated basis*

TABLE 12: MO Energies of $CpTaH_4$ in Its Optimal Geometry (Hartree)[a]

main character of the MOs	$CpTaH_4$	R_5TaH_4	$Cp^{\#}TaH_4$
Cp-Ta−H	−0.38350	−0.38414	−0.37650
Cp-Ta−H	−0.38363	−0.38428	−0.37756
Cp-Ta−H	−0.41898	−0.42357	−0.40990
Cp-Ta−H	−0.41929	−0.42390	−0.41672
Ta−H	−0.43591	−0.43860	−0.42132
Cp-Ta−H	−0.48454	−0.48689	−0.46552
Cp-Ta	−0.61557	−0.61964	−0.64447
Ta	−1.85063	−1.84973	−1.82203
Ta	−1.85064	−1.84974	−1.82203
Ta	−1.86119	−1.85650	−1.82243
Ta	−3.28061	−3.27955	−3.25087

[a] The MOs of $CpTaH_4$ corresponding to C−C and C−H bonds have been omitted for the sake of simplicity.

TABLE 13: Geometrical Parameters of the $Cp^{\#}$ EGP[a]

distances		angles		dihedral angles	
$C_1^{\#}X$	1.205				
$C_2^{\#}X$	1.207	$C_2^{\#}XC_1^{\#}$	72.1		
$C_3^{\#}X$	1.207	$C_3^{\#}XC_1^{\#}$	72.1	$C_3^{\#}XC_1^{\#}C_2^{\#}$	180.0
$C_4^{\#}X$	1.203	$C_4^{\#}XC_2^{\#}$	72.0	$C_4^{\#}XC_2^{\#}C_1^{\#}$	180.0
$C_5^{\#}X$	1.203	$C_5^{\#}XC_3^{\#}$	72.0	$C_5^{\#}XC_3^{\#}C_1^{\#}$	180.0

[a] They coincide with the positions of the reduced system R_5 on which the basis set is defined. This geometry is taken from the optimal structure of $CpTaH_4$. X is the center of the Cp ligand. The numbers of the pseudo-carbons refer to the numbering on Scheme 4.

TABLE 14: Geometrical Parameters for the $CpTaH_4$, $Cp^{\#}TaH_4$, and $ClTaH_4$ Molecules[a]

	$CpTaH_4$	$Cp^{\#}TaH_4$	$ClTaH_4$
XTa	2.130	2.130*	2.373
C_1XTa	89.7	89.7*	
C_1XTaH_1	0.0	0.0*	
TaH_1	1.775	1.797	1.750
TaH_2	1.790	1.799	1.750
TaH_{3-4}	1.780	1.798	1.750
$XTaH_1$	113.3	113.9	117.2
$XTaH_2$	116.4	114.8	117.2
$XTaH_{3-4}$	114.6	114.0	117.2
H_2XTaH_1	180.0	180.2	180.0
$H_{3-4}XTaH_1$	± 88.4	±89.7	±90.5

[a] The geometry features of the Cp group were previously indicated in Table 13.

TABLE 15: Mulliken Population Analysis for $CpTaH_4$

$CpTaH_4$	R_5TaH_4	$Cp^{\#}TaH_4$
$[CH]_1$: 4.990	C_1: 0.983	C_1: 0.954
$[CH]_{2-3}$: 4.982	C_{2-3}: 0.977	C_{2-3}: 0.953
$[CH]_{4-5}$: 4.976	C_{4-5}: 0.968	C_{4-5}: 0.932
Ta: 12.410	Ta: 12.420	Ta: 12.364
H_1: 1.167	H_1: 1.172	H_1: 1.221
H_2: 1.168	H_2: 1.180	H_2: 1.230
H_{3-4}: 1.169	H_{3-4}: 1.176	H_{3-4}: 1.226

TABLE 16: *p* Parameters Used for the Determination of the Nonlocal Potentials for $Cp^{\#}$ [a]

exponents
3.000
1.500
0.750
0.375

[a] The Gaussian functions are located on each $C^{\#}$ center.

set. The best results were obtained with one p shell on each $C^{\#}$. The energies of the delocalized MVPOs and the Mulliken population analysis of the reduced molecule R_5TaH_4 are reported in Tables 12 and 15, respectively. Good agreement with reference calculations is clearly observed. Thus, a single p shell is sufficient to reproduce the 11 pertinent localized MOs. The Cartesian Gaussian functions which define W_{EGP} correspond to p symmetry, and they are located on each $C^{\#}$ (see Table 16). The $(C^{\#})_5$ geometrical parameters given in Table 14 coincide with the $(C)_5$ ones in the optimal geometry of $CpTaH_4$. In the following, the symbolic notation $Cp^{\#}$ will replace the five $C^{\#}$ together. The ability of the operator to reproduce the MO energies and the atomic charges is compared with the reference calculation in the third column of Tables 12 and 15.

As concerns the geometrical parameters, results relative to $ClTaH_4$ are added (Table 14), to compare our method with models in which the cyclopentadienyl ligand is replaced by a chlorine, according to the model proposed by Steigerwald and Goddard.[1] This model has been widely used in previous work in order to reduce the computational effort necessary for a complete investigation of PES since it is out of reach because of the size of system to study.[17−19]

Numerical experimentation shows that an acceptable accuracy on the valence molecular spectrum and the optimized geometry is obtained with our operator. However, a slight tendency is observed: the Ta−H distances are overestimated with the $Cp^{\#}$ EGP. We also checked the agreement between the force constants of $CpTaH_4$ and $Cp^{\#}TaH_4$. At this stage it is to be noted that the PES of this complex is very flat. Indeed, elongation or reduction of the bond length induce weak variations in energy. For instance, the bending force constant of one HTaH angle is found to be about 9×10^{-5} mdyn·Å·rad^{-2}. This finding implies that our operator is able to reproduce subtle effects. For comparison, other calculations have been performed with other basis sets and atomic pseudopotentials (ECP) on the transition metal atom. We computed, with respect to the reference calculation, the mean relative deviation for bond lengths obtained with these different calculations. The mean relative deviation (in %) on a variable d is calculated as

$$d = \frac{1}{N}\sum_{i=1}^{N} \frac{|d_i - d_i^{\#}|}{d_i} \times 100$$

where N is the number of samples. These quantities are presented in Table 17. The mean relative deviations observed with our work are in the same range as those given by

TABLE 17: Mean Relative Deviations (in %) of the M−H Bond Length and HMH Angles for the Optimized Geometries of $CpMH_4$ Obtained with Various Molecular or Atomic Pseudopotentials with Respect to the Reference Calculation (Durand and Barthelat Pseudopotentials for M, Where M = Ta or Nb)

			$CpMH_4$	
	M	$Cp^{\#}MH_4$	Dolg ECP[18]	Seijo ECP[19]
bond	Ta	0.94	0.52	0.82
	Nb	1.00	0.60	0.50
angle	Ta	0.80	0.63	0.01
	Nb	6.00	2.60	5.40

TABLE 18: Mulliken Population Analysis.

$CpNbH_4$	$Cp^{\#}NbH_4$	$ClNbH_4$
$[CH]_1$: 4.996	$[CH]_1$: 0.903	Cl: 7.34
$[CH]_1$: 4.974	$[CH]_1$: 0.952	
$[CH]_{2-3}$: 4.969	$[CH]_{2-3}$: 0.930	
Nb: 12.727	Nb: 12.691	Nb: 12.42
H_1: 0.976	H_1: 1.078	H_1: 1.061
H_2: 1.195	H_2: 1.223	H_2: 1.061
H_{3-4}: 1.081	H_{3-4}: 1.147	H_{3-4}: 1.061

TABLE 19: Geometrical Parameters for the $CpNbH_4$ Structure (Units: Same Convention as in Table 2)

	$CpNbH_4$	$Cp^{\#}NbH_4$	$ClNbH_4$[a]
XNb	2.219	2.219*	2.382*
C_1XNb	93.1	93.1*	
C_1XNbH_1	1.0	1.0*	
NbH_1	1.714	1.747	1.722
NbH_2	1.812	1.812	1.722
NbH_{3-4}	1.752	1.770	1.722
$XNbH_1$	103.8	107.0	119.9
$XNbH_2$	133.5	129.1	119.9
$XNbH_{3-4}$	108.2	112.4	119.9
H_2XNbH_1	181.6	176.4	180.0
$H_{3-4}XNbH_1$	± 70.0	±76.5	±90.0

[a] X = Cl.

calculations on the full $CpTaH_4$ molecule with different atomic pseudopotentials. Since the utilization of atomic pseudopotentials is almost compulsory in large molecules, the differences between two atomic pseudopotentials give us the maximum precision required for our method.

Moreover, comparison with calculations where the Cp ligand is replaced by a chlorine speaks in favor of our method. The symmetry for the optimized structure of $Cp^{\#}TaH_4$ is C_s, like the reference $CpTaH_4$ complex, whereas the $ClTaH_4$ complex clearly has C_{4v} symmetry, with identical Ta−H bond lengths too small and identical XTaH angle too large as compared to the reference geometry. As expected, a model with Cl atom fails to reproduce the $CpTaH_4$ geometry and moreover, it is more time-consuming than our procedure.

5.2. Transferability. Again, to demonstrate the usefulness of our method, we must make sure of the transferability of our effective group operator. In other words, can we employ the $Cp^{\#}$ EGP extracted on $CpTaH_4$ in ab initio calculations involving another metal? To answer this question we decided to test the transferability of the $Cp^{\#}$ EGP on $CpNbH_4$. From the optimized geometry obtained for $CpNbH_4$, it can be stated that this complex possesses an almost piano-stool geometry. It must be pointed out that this structure is notably different from the one obtained for $CpTaH_4$. So this step is a crucial test for our potential. Results shown in Tables 18 and 19 indicate that our method is successful, since we obtain good accuracy with respect to the reference calculation. The $Cp^{\#}$ potential is able to reproduce the valence molecular spectrum (occupied and virtual orbitals, see Figure 2). For instance, the energy gap between

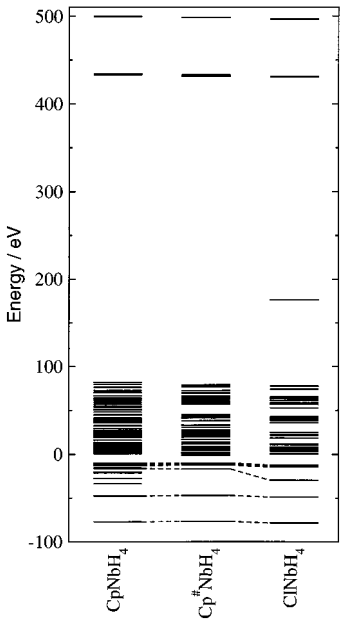

Figure 2. Energies (hartree) of the EGPs of $CpNbH_4$, $Cp^{\#}NbH_4$ and $ClNbH_4$ in their respective optimal geometry. The dashed lines correlate occupied orbitals with analogous character.

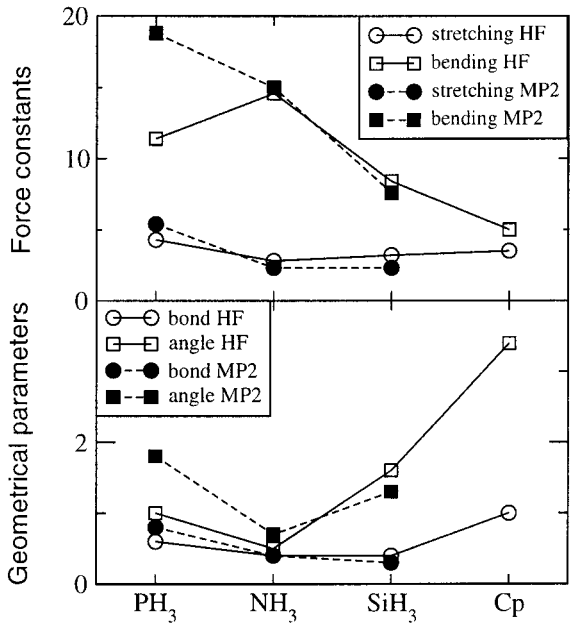

Figure 3. Mean relative deviation of the geometrical parameters and force constants at the HF or MP2 level of calculation.

the HOMO and LUMO is in good agreement: 0.33843 hartree in $CpNbH_4$ compared to 0.34160 hartree in $Cp^{\#}NbH_4$. The $Cp^{\#}$ EGP is also able to describe the optimal structure of $CpNbH_4$. As a matter of fact, even if discrepancies exist between angles of the reference structure and those obtained with $Cp^{\#}$ and even if the Nb−H distances remain slightly too large, the overall trend is respected. In Table 17 mean relative deviations obtained using other atomic pseudopotentials are compared. They are of the same order of magnitude as those obtained with our results. Our method gives on the whole quite accurate geometries with respect to the other tests we performed.

6. Conclusion

The goal of the present contribution is not only the reduction of an ab initio calculation. We have at the back of our mind the idea of simplifying an apparently complex problem by the identification of the irrelevant information in the framework of that problem. From the postulates of quantum mechanics, the wave function can be seen as a catalog of information. This is the case of the Hartree−Fock wave function, which is delocalized over all the molecule. Is it necessary to dispose of so much information? We believe that physically based simplifications can help to rationalize the analysis of a quantum mechanical calculation. This is the underlying idea of the EGP method. Indeed, in the molecular case, the irrelevant information is identified as functional groups which do not participate in the studied process, that is, spectator groups. This treatment provides a more readable Hartree−Fock solution, without a significant loss in accuracy. As a matter of fact, although the spectator groups are replaced by fictitious systems with a reduced number of electrons and nuclei, the electronic wave function and energy of the active part are not significantly altered. Applications to groups involved in covalent and donor−acceptor bonds have been presented. The parametrization of EGPs for functional groups such as SiH_3, PH_3, NH_3 and C_5H_5 was carried out, and systematically checked. The silyl, phosphine and ammonia EGPs are one-center anisotropic potentials, while the effect of the π-system of a cyclopentadienyl fragment is better mimicked by a multicenter potential. We underline that the greater part

TABLE 20: n = Number of Electrons, N_{bf} = Number of Basis Functions, N_s = Number of Shells, and t = CPU time (s) Required for the Hartree−Fock Calculation (without Symmetry) of the Optimal Geometry of Each System on a PentiumII PC under the Linux System

	Si_2H_6	$SiH_3Si^{\#}$	Si_5H_{12}	$SiH_3SiSi_3\#$	$CpTaH_4$	$Cp^{\#}TaH_4$
n	14	8	32	14	42	22
N_{bf}	56	32	125	53	107	72
N_s	28	16	61	25	57	32
t	71	5	840	36	723	127

of the present tests have been performed on systems in which all the active part is very strongly intertwined with the spectator groups. The EGPs were thus submitted to severe tests in the framework of HF and MP2 theories and the results are always in good agreement with those of full ab initio calculations. The mean relative deviation of the geometrical parameters and force constants of the EGP results, with regard to the complete molecule calculations, provides a synthetic overview of the present work. This quantity is reported in Figure 3. There is no major difference between HF and MP2 results, though the mean error on the PH_3 bending force constants differs from 7%. As stated above, this is mainly due to the less good results obtained for BH_3 PH_3. As for errors on the geometries obtained with $Cp^{\#}$, they are only slightly higher than with the other EGPs. This can be explained by the flatness of the potential energy surface of the studied system. Furthermore, finding almost identical results with different atomic pseudopotentials is already a hard task.

From a more pragmatic point of view, the interesting consequence is the reduction of the cost of a Hartree−Fock calculation, as can be seen in Table 20. The most striking example is Si_5H_{12}. Fourteen minutes are needed for the full ab initio calculation, while the calculation with the $Si^{\#}$ EGP requires only 36 s. As a matter of fact, the problem is reduced by 36 electrons and 72 basis functions.

Although methodological improvements and further tests are needed, we believe that the EGP method is promising and could be applied to a wide variety of chemical problems. They are extracted at an ab initio level and can be included in any quantum mechanics program.

Quantum mechanics is imperatively needed for describing the breaking and making of chemical bonds, electron transfer processes, or local electronic excitations. Despite both methodological improvements in the resolution of SCF equations, such as the linear scaling methods,[20] and the increase in computer speed, studies of large systems such as enzymes, proteins, dendrimers, organized molecular systems, ... are hardly feasible, even with semiempirical approaches. Recent work show that there is a need for elucidating chemical problems in the field of applied reseach.[21] There is thus a strong interest in developing methods which could extend the applicability of ab initio approaches to large molecular systems. In the so-called hybrid QM/MM methods, the active part of a molecule is treated quantum mechanically (QM) while the inactive part is described with molecular mechanical (MM) potentials. The difficulty arises for the description of the intramolecular frontier between the QM and MM parts.[22] The present EGP scheme could be integrated as a part of QM/MM methods. It could resolve both the lack of steric interactions of the EGP part with the active part (as in the IMOMM method[23]) and the problem of frontier bonds in hybrid methods. Such an hybrid QM/QM#/MM tool could be very powerful for the study of large problems in which the quantum mechanical approach is needed.

Acknowledgment. The authors acknowledge support from the ECOS program PM098P01.

References and Notes

(1) Steigerwald, M. L.; Goddard, W. A., III. *J. Am. Chem. Soc.* **1984**, *106*, 308−311.

(2) Barthelat, J.-C.; Chaudret, B.; Daudey, J.-P.; de Loth, Ph.; Poilblanc, R. *J. Am. Chem. Soc.* **1991**, *113*, 9896−9898.

(3) Frisch, M. J.; Trucks, G. W.; Schlegel, H. B.; Scuseria, G. E.;. Robb, M. A.; Cheeseman, J. R.; Zakrzewski, V. G.; Montgomery, J. A.; Stratmann, R. E.; Burant, J. C.; Dapprich, S.; Millam, J. M.; Daniels, A. D.; Kudin, K. N.; Strain, M. C.; Farkas, O.; Tomasi, J.; Barone, V.; Cossi, M.; Cammi, R.; Mennucci, B.; Pomeli, C.; Adamo, C.; Clifford, S.; Ochterski, J.; Petersson, G. A.; Ayala, P. Y.; Cui, Q.; Mokoruma, K.; Malick, D. K.; Rabuck, A. D.; Raghavachari, K.; Foresman, J. B.; Cioslowski, J.; Ortiz, J. V.; Stefanov, B. B.; Liu, G.; Liashenko, A.; Piskorz, P.; Komaromi, L.; Gomperts, R.; Martin, R. L.; Fox, D. J.; Keith, T.; Al-Laham, M. A.; Peng, C. Y.; Nanayakkara, A.; Gonzalez, C.; Challacombe, M.; Gill, P. M. W.; Johnson, B. G.; Chen, W.; Wong, M. W.; Andres, J. L.; Head-Gordon, M.; Replogle, E. S.; Pople, J. A. *Gaussian 98*; Gaussian, Inc.: Pittsburgh, PA, 1998.

(4) Durand Ph.; Barthelat, J.-C. *Theor. Chim. Acta* **1975**, 38, *283*−*302*. Barthelat, J.-C.; Durand, Ph. *Gazz. Chim. Ital.* **1978**, *108*, 225-*236*.

(5) Barthelat, J.-C. Private communication.

(6) The basis sets used in this work and the Ta and Nb pseudopotentials are available upon demand.

(7) *Handbook of Chemistry and Physics*, 77th ed.; Lide, D. R., Ed.; CRC Press: Boca Raton, FL, 1996.

(8) See, for example: (a) Grev, R. S.; Scheafer, H. F., III. *J. Chem. Phys.* **1992**, *97*, 8389−8406. (b) Onida, G.; Andreoni, W. *Chem. Phys. Lett.* **1995**, *243*, 183−189. (c) Zhang, R. Q.; Costa, J.; Bertran, E. *Phys. Rev. B* **1996**, *53*, 7847-*7850*.

(9) Canham, L. T. *Appl. Phys. Lett.* **1990**, *57*, 1046−1048.

(10) Costa, J.; Roura, P.; Sardin, G.; Morante, J. R.; Bertran, E. *Phys. Rev. B* **1994**, *50*, 18124−18133.

(11) A specific theoretical study of Lewis acid−base complexes of the kind NH_3 BH_3 can be found in: Jonas, V.; Reetz, M. T. *J. Am. Chem. Soc.* **1994**, *116*, 8741−8753.

(12) Chaillet, M.; Dargelos, A.; Marsden, C. J. *New J. Chem.* 1994 *18*, 693−700.

(13) Anane, H.; Boutalib, A.; Nebot-Gil, I.; Tomas, F. *Chem. Phys. Lett.* **1998**, *287*, 575−578.

(14) Thorne; Lovas, F. J. *J. Chem. Phys.* **1983**, *78*, 167−171.

(15) For molecular orbital understanding of this kind of system, see for example: Albright, T. A.; Burdett, J. K.; Whangbo, M. H. *Orbital interactions in chemistry*; Wiley-Interscience: New York, 1985.

(16) Kubacek, P.; Hoffmann, R.; Havlas, Z. *Organometallics* **1982**, *1*, 180−188.

(17) Abou el Makarim, H.; Barthelat, J.-C. Private communication.

(18) Andrae, D.; Haeussermann, U. H.; Dolg, M.; Stoll, H.; Preuss, H. *Theor. Chim. Acta* **1990**, *77*, 123-*141*.

(19) Barandiaran, Z.; Seijo, L.; Huzinaga, S. *J. Chem. Phys.* **1990**, *93*, 5843-*5850*.

(20) Kudin, K. N.; Scuseria, G. *Chem. Phys. Lett.* **1998**, *283*, 61−68.

(21) Jang, Y. H.; Blanco, M.; Dasgupta, S.; Keire, D. A.; Shively, J. E.; Goddard, W. A., III. *J. Am. Chem. Soc.* **1999**, *121*, 6142−6151.

(22) For a critical discussion about the treatment of the frontier bonds, see: Reuter, N.; Dejaegere, A.; Maigret, B.; Karplus, M. *J. Phys. Chem.* **2000**, *104*, 1720−1735.

(23) Maseras, F.; Morokuma, K. *J. Comput. Chem.* **1995**, *16*, 1170−1179.